Journal of Food Safety and Food Quality
Archiv für Lebensmittelhygiene

J. Food Saf. Food Qual. **2026**; 77(2): 50662
https://doi.org/10.31083/JFSFQ50662

Original Research

Development of a Surface-Enhanced Raman Spectroscopy Based Method using Molecularly Imprinted Polymers for the Detection of Trichlorfon and Cypermethrin in Fruits and Vegetables

Shuai Tang[1,2], Hong Chang[3], Gao-hao Tan[4], Hai-rong Cen[5], Qiu-an Mo[6,*]

[1]Haikou Xiuying Center for Disease Prevention and Control, 570311 Haikou, Hainan, China
[2]Haikou Xiuying District Maternal and Child Health Institution, 570311 Haikou, Hainan, China
[3]Business and Technology Department, Hainan Academy of Inspection and Testing, 570100 Haikou, Hainan, China
[4]Institute of Food Testing, Hainan Academy of Inspection and Testing, 570100 Haikou, Hainan, China
[5]Qionghai Branch of Hainan Academy of Inspection and Testing, 571442 Qionghai, Hainan, China
[6]Danzhou Branch of Hainan Academy of Inspection and Testing, 571700 Danzhou, Hainan, China
*Correspondence: 394291440@qq.com (Qiu-an Mo)
Academic Editor: Corinna Kehrenberg
Submitted: 3 February 2026 Revised: 18 March 2026 Accepted: 23 March 2026 Published: 28 April 2026

Abstract

Background: Excessive residues of organophosphorus pesticide pose a serious threat to consumer health and negatively impact the export trade of agricultural products in China. Therefore, establishing a rapid, accurate and reliable multiresidue detection method for organophosphorus pesticides to safeguard consumer health is highly necessary. **Methods**: This study aimed to develop a combined detection method integrating surface-enhanced Raman spectroscopy (SERS) with molecularly imprinted polymer (SERS-MIP) technology. Quantitative analysis of two pesticides, trichlorfon and cypermethrin, as examples, enables rapid detection of pesticide residues in fruits and vegetables. The effects of four fruits and vegetables (oranges, tangerines, leeks, and spinach) on the detection of two pesticide residues were also investigated, with a focus on matrix effects on the SERS-MIP combined technique. **Results**: The limit of detection (LOD) for trichlorfon in oranges and tangerines was 1.27 µg/kg, with recovery rates ranging from 95.2% to 101.4%. The LOD for cypermethrin in leeks and spinach was 0.13 µg/kg, with recovery rates ranging from 95.2% to 100.3%. For all four matrices, the method enabled rapid quantitative detection with high specificity and sensitivity, meeting current market demands. **Conclusions**: This approach holds promise for detecting other pesticide residues and provides a useful reference direction for developing rapid pesticide residue testing methods.

Keywords: organophosphorus pesticides; surface-enhanced Raman spectroscopy; molecular imprinting; solid-phase extraction

1. Introduction

Trichlorfon is an organophosphorus insecticide with high efficiency and broad spectrum insecticidal characteristics. It is widely used in agriculture to control chewing mouthparts and biting mouthparts of agricultural, forestry, horticultural pests, underground pests, etc. [1,2]. Cypermethrin is an organochlorine insecticide, mainly used to control lepidoptera pests that occur on crops. It is highly toxic and has a high insecticidal activity against many kinds of pests. It can be applied to various fruit trees, fruits and vegetables, etc., and has a good killing effect on many kinds of pests [1,3]. In agricultural production, these two pesticides are usually used in combination, which has a synergistic effect [4].

At present, the major detection methods for the residues of these two pesticides mainly include chromatography, immunoassay, and sensor-based methods [2,5]. Among these methods, chromatography demands relatively complex sample pretreatment procedures. Additionally, it incurs high costs, requires expensive instrumentation, and necessitates professional technical expertise [6,7]. Immunoassay methods, on the other hand, have a long cycle. The biological activity of antibodies is susceptible to inactivation due to multiple influencing factors [8,9]. Moreover, the preparation of pesticide antibodies involves the synthesis of complete antigens and immunization of animals, which poses challenges for industrial production [10,11]. In most of the current biosensors, biomolecules (such as antibodies and enzymes) are utilized as recognition elements [12]. However, these biomolecules often exhibit poor stability and limited repeatability in detection. Chemical sensors typically rely on the polarity differences of analytes for detection, resulting in a lack of specificity in their detection capabilities [13,14]. Consequently, the development of sensitive materials with specific recognition capabilities for the analytes of interest has emerged as a crucial aspect in the research and development of novel detection methods [15,16].

In recent years, the number of articles published on the application of surface-enhanced Raman spectroscopy (SERS) for detecting pesticide residues has increased exponentially [17–20]. Different pesticides possess distinct

molecular structures and chemical bond configurations, resulting in varying intermolecular forces. These differences can be effectively distinguished through the characteristic peak positions, number of peaks, peak shapes, and peak intensities in SERS spectra. Combined with mathematical modelling, this approach establishes relationships between pesticide concentrations and characteristic peak intensities, thereby enabling both qualitative and quantitative analysis of pesticide residues in fruits and vegetables using SERS technology [4,12]. Lin *et al*. (2018) [21] employed SERS to determine thiabendazole pesticide residues in rapeseed. They established a predictive model that links SERS spectral data to thiabendazole pesticide levels in rapeseed via partial least squares regression.

Molecular imprinting technology mimics the mechanism of antibody-antigen interaction. When the template molecule (imprinting molecule) comes into contact with the functional monomer, multiple interaction sites are formed [11,22]. Through the polymerization process of the crosslinking agent, this interaction is memorized. After the template molecule is removed, stereospecific cavities complementary to the template molecule in terms of spatial structure, size and binding sites are left in the polymer network structure. Such cavities exhibit highly selective recognition characteristics for the template molecule and its analogues [23,24]. In recent years, molecular imprinting has been used as a recognition unit to specifically recognize and bind target molecules, and combined with different types of transducers to produce molecularly imprinted sensors [25,26]. It not only has the advantages of high sensitivity and simple, rapid operation of chemical sensors, but also has the advantages of mechanical stability, thermal stability, long service life and multiple reusability of molecularly imprinted polymers [16,27]. Therefore, it has shown broad application prospects in the field of pesticide residue detection and has become an important research hotspot [11,16].

With the rapid socio-economic development in China, there has been increasing public concern regarding quality of life, particularly heightened attention toward food quality and safety [7,12,15]. However, due to the extensive application of organophosphorus pesticides (OPs) in crop production and cultivation, the issue of OP pesticide residues exceeding maximum limits has emerged as a significant concern [23–25]. Although China has established stringent maximum residue limits (MRLs) for organophosphorus pesticides in fruits and vegetables, fruits, and other agricultural commodities, the misuse and overuse of these chemicals, along with violations involving restricted or banned OPs, remain prevalent. Moreover, there has been an increasing frequency of detecting multiple OP residues in produce [13,22,23]. The problem of excessive OP pesticide residues not only poses serious threats to consumer health but also adversely affects the export trade of Chinese agricultural products. Therefore, it is imperative to establish rapid, accurate, and reliable multi-residue detection methods for organophosphorus pesticides to ensure public health protection and enhance food safety monitoring [8,23,25].

Based on molecularly imprinted technology, this study establishes a rapid and effective method for the detection of multiple trace-level organophosphorus pesticide residues by combining molecularly imprinted solid-phase extraction with high-performance liquid chromatography (MISPE-HPLC). The proposed method not only significantly enhances detection sensitivity and lowers the limits of detection, but also represents a novel exploration into the application of molecularly imprinted solid-phase extraction technology for multi-residue analysis of organophosphorus pesticides.

This manuscript is the first to employ surface-enhanced Raman spectroscopy for the qualitative and quantitative analysis of two pesticides, trichlorfon and cypermethrin. Subsequently, by integrating surface-enhanced Raman spectroscopy with molecularly imprinted polymer technology, it conducts pesticide residue detection in actual vegetable samples. This approach overcomes the limitations of conventional SERS detection and offers broad research value and application prospects for achieving highly specific and sensitive SERS detection.

2. Materials and Methods

2.1 Materials

Trichlorfon (purity 90%), cypermethrin (purity 4.5%), methacrylic acid, ethylene glycol dimethacrylate, azobisisobutyronitrile, methanol, glacial acetic acid, chloroform, silver nitrate, trisodium citrate and acetone were purchased from Shanghai Aladdin Biochemical Technology Co., Ltd. High-purity nitrogen (99.999%) was purchased from Hainan Jiateng Chemical Gas Co., Ltd. Oranges, mandarins, spinach and leeks were purchased from Nanguo Supermarket, Haikou, Hainan Province.

2.2 Preparation and Performance of Mixed Template Molecularly Imprinted Polymers for Trichlorfon and Cypermethrin

2.2.1 Preparation of Molecularly Imprinted Polymers for Trichlorfon and Cypermethrin

The template molecules (0.2867 g of Trichlorfon and 9.2244 g of Cypermethrin) were dissolved in 12 mL chloroform in a three-neck flask, followed by the addition of 2.756 g of methacrylic acid (8 mmol) as the functional monomer. The mixture was stirred at room temperature for 30 minutes to ensure thorough mixing. Ethylene glycol dimethacrylate (3.964 g, 20 mmol) was added as the crosslinking agent, followed by 400 mg of azobisisobutyronitrile as the initiator. The reactions were configured with 0.5 mmol of template monomer, a template:functional monomer:crosslinker ratio of 1:4:20 (n:m:n), 0.44 mmol of initiator, and a pore-forming agent consisting of a mixed solution of acetonitrile/methanol (volume ratio = 3/1). After thorough mixing, the flask was sealed and sonicated for 15 mins. After nitro-

gen gas was introduced for 15 minutes to remove oxygen, the flask was sealed and placed in a 60 °C water bath for 24 h [11,12].

Soxhlet Extraction for Removal of Pesticide Template Molecules from the Polymer: After the polymerization process was completed, an amber-colored solid was obtained. The solid was thoroughly ground in a mortar and sieved through a 200-mesh screen. The resulting powder was tightly wrapped in a filter paper thimble and placed into the extraction chamber of a Soxhlet apparatus. A mixture of methanol and glacial acetic acid (120 mL:40 mL, 3:1 v/v) was used as the extraction solvent. The extraction system was assembled and heated in a water bath at 93 °C. Siphoning occurred approximately every 20 min. After 12 h of continuous extraction, the thimble was removed. The extracted polymer was then washed with methanol until neutral pH was achieved and dried in an oven at 50 °C for 12 h to obtain the final molecularly imprinted polymer (MIP) [15,16,22].

The non-imprinted polymer (NIP) was prepared following the same procedure, except that no pesticide template molecule was added during the polymerization.

2.2.2 Scanning Electron Microscopy (SEM) Characterization of Trichlorfon, Molecularly Imprinted Polymer (MIP), and Non-Imprinted Polymer (NIP)

The surface morphologies of trichlorfon, the molecularly imprinted polymer (MIP), and the non-imprinted polymer (NIP) were characterized using scanning electron microscopy (SEM) to evaluate structural and topological features. A drop of nanometer compound was taken from the copper-covered network with membrane, subjected to natural air and 2% phosphotungstic acid dye for 30 min in the copper network carrying the nanometer compound. A filter paper was used to absorb the excess dye. Then, the sample was scanned with a transmission electron microscope using an acceleration volt-age of 80 kV [11,12].

2.2.3 Fourier Transform Infrared (FTIR) Spectroscopy Analysis

FTIR spectroscopy was employed to characterize trichlorfon, MIP, and NIP. By comparing the stretching vibration peaks of specific functional groups in the infrared spectra, the elution efficiency of the pesticide molecules was evaluated. The samples' infrared spectrum analysis was performed using the KBr method, with a wave number in the range of 400 to 4000 cm^{-1}. Scanning was conducted for 32 times at a resolution of 4 cm^{-1}. This analysis also helped determine whether chemical bonding occurred between the trichlorfon molecules and the functional monomer, methacrylic acid [28,29].

2.2.4 Adsorption Kinetics Experiments

A standard aqueous solution of trichlorfon or cypermethrin at a concentration of 300 mg/L was accurately prepared. All experiments were performed in triplicate: 20 mg of molecularly imprinted polymer (MIP) was weighed into seven 50-mL volumetric flasks, followed by the addition of 10 mL of the 300 mg/L trichlorfon or cypermethrin standard solution. The flasks were shaken in an incubator at room temperature for periods ranging from 5 to 240 mins. After shaking, the mixtures were centrifuged at 4000 rpm for 30 mins. The supernatant was then carefully collected, and its absorbance was measured at 190 nm using a UV-Vis spectrophotometer. The same procedure was applied in parallel to evaluate the non-imprinted polymer (NIP) [10,12].

2.2.5 Equilibrium Binding Experiments of Molecularly Imprinted Polymers

To evaluate the adsorption performance of the two types of molecularly imprinted polymers, equilibrium binding studies were conducted with trichlorfon and cypermethrin. Exactly 20 mg of MIP was weighed into a 50-mL volumetric flask, and 10 mL of trichlorfon or cypermethrin solution at concentrations ranging from 0 to 300 mg/L was added. The mixtures were oscillated at room temperature for 4 hours and then centrifuged at 4000 rpm for 15 minutes. The supernatant was filtered through a 0.22 µm aqueous-phase membrane, and a 50 µL aliquot was injected for HPLC analysis at a detection wavelength of 200 nm [15,23].

2.3 Detection of Trichlorfon and Cypermethrin Pesticide Residues in Food Using MIP Combined With SERS Technology

2.3.1 Preparation of Silver Nanoparticles (AgNPs) Synthesis Protocol

Measure 15 mL of 0.01 mol/L silver nitrate standard solution into a 150 mL volumetric flask. Dilute to volume with ultrapure water. Add a clean, dry magnetic stir bar and heat while stirring at 100 °C. Once boiling commences with uniform bubble formation, slowly add 3 mL of 1% trisodium citrate solution dropwise while maintaining stirring and heating for approximately 30 minutes. Cease heating and allow the mixture to cool naturally to room temperature. Take 40 g of the solution and centrifuge at 3500 rpm for 2 min to remove larger silver nanoparticle particles. Ultrasonically disperse the supernatant for 20 min to ensure thorough mixing, yielding the AgNPs. Store away from light [19,30].

2.3.2 Preparation of Standard Solutions of the Two Pesticides

Five silver nitrate solutions were prepared at different concentrations: 0.2, 0.6, 1.0, 1.4, and 1.8×10^{-3} mol/L. From each concentration of silver nitrate, 150 mL was taken to synthesise AgNPs as SERS-enhanced substrates. Five sodium chloride solutions were also prepared at concentrations of 0.2, 0.6, 1.0, 1.4, and 1.8×10^{-2} mol/L, (5 mL each) for subsequent use. The 10^{-2} mol/L stock standard

solutions of trichlorfon and cypermethrin were serially diluted with methanol to obtain concentrations ranging from 10^{-2} to 10^{-8} mol/L. The diluted solutions were stored in sealed volumetric flasks to provide standard solutions of the two pesticide molecules at various concentrations [31].

2.3.3 Acquisition of Raman and SERS Spectra

Raman and SERS spectra of the trichlorfon and cypermethrin standard solutions were acquired using a HORIBA HR Evolution microconfocal Raman spectrometer. Prior to the experiment, the instrument was calibrated using a silicon wafer. A 5 µL aliquot of AgNPs was mixed with 5 µL of the test solution on a microscope slide, thoroughly mixed, and the slide was placed on the stage after 2 min. Exposure to light was avoided throughout. Measurements were performed using the Raman spectrometer to collect the spectra. This method was applied to each concentration of the pesticide solutions. Unless otherwise specified, the spectral acquisition parameters were as follows: laser wavelength, 532 nm; laser intensity, 50%; laser spot diameter, 200 µm; grating, 600 grooves/mm (centre wavelength 500 nm); and a 50× objective lens on the confocal microscope. Ten SERS spectra were collected for each concentration [19,30,32].

2.3.4 Sample Preparation

Common leeks, which may retain residues of trichlorfon and cypermethrin, were selected as the actual samples for testing. The leek samples were spiked with known amounts of both pesticides. By combining the MIPs to adsorb the pesticide molecules with the prepared AgNPs as the SERS enhancement substrate, SERS spectra were acquired from the pesticide-contaminated leek samples. The leeks were rinsed with ultrapure water, air-dried in a fume hood for 30 min, immersed in the pesticide solutions for 5 min, removed and then left in a cool place for 24 h. This procedure ensured that the spiked pesticide concentrations closely approximated real-world contamination levels [17,33].

2.3.5 Acquisition of SERS Spectra

Three grams of each of the two prepared pesticide-specific molecularly imprinted polymers (MIPs) were weighed and dissolved in 3 mL of methanol. Chopped leeks were placed on a glass slide, 5 µL of the molecularly imprinted polymer solution was added, and the MIPs were allowed to adsorb fully onto the sample and dry. Subsequently, 5 µL of AgNPs was added. After 2 min, surface-enhanced Raman spectroscopy signals were collected from ten uniformly distributed points on the sample surface. Measurements were taken multiple times at each concentration, and the average value was selected once the signal intensity has stabilised; this average was used as the final measurement result. The instrument parameters were as follows: laser wavelength, 532 nm; laser intensity, 50%; laser spot diameter, 200 µm; grating centred at 500 nm; and a 50× objective lens on the confocal microscope [30,34].

2.4 Data Processing

All experiments were performed in triplicate. Data were analyzed using SPSS 22.0 software (IBM Corp., Armonk, NY, USA). One-way ANOVA and paired sample *t*-tests were employed to assess significant differences between groups. A p-value < 0.05 was considered statistically significant, <0.01 as highly significant, and >0.05 as not significant. Figures were generated using Origin 8.5 (IBM Corp., Armonk, NY, USA).

3. Results and Discussion

3.1 Characterization of Molecularly Imprinted Polymers

3.1.1 Scanning Electron Microscopy (SEM) Analysis

The molecularly imprinted polymers (MIPs) synthesized using trichlorfon and cypermethrin as template molecules, along with the non-imprinted polymer (NIP), were characterized by SEM. As shown in Fig. 1, molecularly imprinted polymer shown in the left figure has a microspherical surface with a large specific surface area. It is porous and has a rough, uneven texture. This morphological difference can be attributed to the interactions between the pesticide template molecules and the functional monomer during polymerization, leading to the formation of numerous microspheres complementary in size and shape to the templates [23,25]. In contrast, the NIP, synthesized in the absence of template molecules, lacks such specific cavities, resulting in a comparatively smoother surface with fewer pores.

3.1.2 Fourier Transform Infrared (FTIR) Spectroscopy

The FTIR spectra of the MIP, NIP, and trichlorfon are shown in Fig. 2. In the spectrum of MIP (Fig. 2A), the absorption peak at 1240.84 cm^{-1} corresponds to the stretching vibration of P=O [17]. Both the MIP (Fig. 2A) and NIP (Fig. 2B) show absorption near 1730 cm^{-1}, attributed to the C=O stretching vibration. 2962.02 corresponds to C-H stretching vibrations of methyl (-CH_3) or methylene (-CH_2) groups. A broad absorption peak observed at 3503.93 cm^{-1} in the MIP spectrum (Fig. 2C) indicates the presence of O–H stretching vibrations due to intermolecular hydrogen bonding. This suggests that the P=O group of trichlorfon interacted with the –OH group of methacrylic acid, confirming successful binding between the mixed templates and the functional monomer during MIP synthesis [11,15]. The similarity between the FTIR spectra of the MIP and NIP (Fig. 2A,B) indicates analogous molecular structures, confirming the effective removal of template molecules from the MIP.

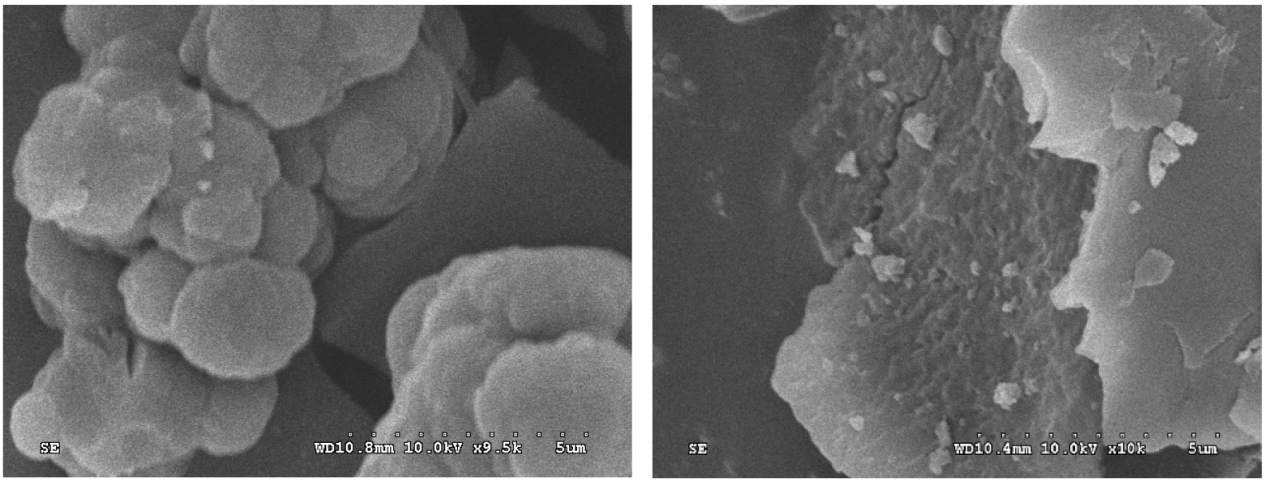

Fig. 1. Scanning electron micrographs of molecularly imprinted polymers. Scanning electron micrographs of molecularly imprinted polymers (A) (×10,000) and non-imprinted polymers (B) (×10,000).

3.1.3 Adsorption Kinetics

The adsorption capacity was measured at different time intervals (Fig. 3). The results demonstrate that the adsorption capacity of the MIP increased over time, reaching a maximum value of 32.24 mg/g, indicating high adsorption affinity for trichlorfon [23,25].

As shown in Fig. 3, after 30 minutes of shaking, the adsorption capacities of the common MIP toward trichlorfon and cypermethrin were 17.4 mg/g and 18.9 mg/g, representing 61.3% and 62.4% of the saturated adsorption capacity, respectively. Adsorption equilibrium was essentially reached within 180 mins. These results suggest that the common MIP exhibits rapid adsorption kinetics for organophosphorus pesticides and can be effectively used as a sorbent in matrix solid-phase dispersion extraction for rapid extraction of such pesticides from samples [24,26].

3.2 Specific Adsorption Detection by MIPs

The specific adsorption performance of Tri-MIPs and Cyp-MIPs was verified using solutions of different pesticide molecules. Although trichlorfon and cypermethrin are both benzene-containing compounds with similar molecular structures, cross-adoption experiments were conducted followed by SERS detection. After elution, Tri-MIPs, Cyp-MIPs, and the corresponding non-imprinted polymers (NIPs) were separately exposed to 1×10^{-6} mol/L solutions of trichlorfon, cypermethrin, and an equimolar mixture of the two. Following 1.5 h of adsorption, SERS signals were acquired using the AgNP-enhanced substrate, as shown in Fig. 4A. No characteristic peak signals for trichlorfon or cypermethrin were detected with any of the three polymers (Tri-MIPs, Cyp-MIPs, or NIPs) when exposed to structurally similar pesticide. This indicates that the prepared MIPs do not bind specifically to compounds with similar structures. After elution, Tri-MIPs, Cyp-MIPs, and the corresponding NIPs were separately exposed to 1×10^{-6} mol/L solutions of trichlorfon, cypermethrin, and an equimolar mixture of both at 1×10^{-6} mol/L. Following 1.5 h of adsorption, SERS signals were acquired using the AgNP-enhanced substrate, with results shown in Fig. 4B. Tri-MIPs clearly exhibited the characteristic peaks of trichlorfon at 996 cm^{-1} and 1595 cm^{-1}, whereas Cyp-MIPs exhibited those of cypermethrin at 719 cm^{-1} and 1596 cm^{-1}. Both polymers successfully adsorbed their respective target pesticide molecules. Even when the concentrations of both pesticides were increased to 1×10^{-2} mol/L, the NIPs still showed no characteristic peaks, confirming that NIPs lack specific adsorption capability for these pesticides. In contrast, only the MIPs possess numerous specific binding sites. These sites can be occupied solely by pesticide molecules that match their spatial shape and functional group arrangement, thereby confirming the specific binding capability of the MIPs.

3.3 Spiked Sample Testing

To evaluate the feasibility of the SERS-MIP method for rapid pesticide detection and to validate the practical application of the prepared MIPs and AgNP-enhanced substrates in real vegetable samples, spiked samples were analysed. Chinese chives were selected as the matrix for spiked recovery experiments. SERS spectra were acquired ten times for each spiked concentration.

Fig. 5A shows the SERS spectra of trichlorfon spiked into leeks at different concentrations. Spectra a–e correspond to trichlorfon spiking concentrations of 1×10^{-4}–1×10^{-8} mol/L, respectively. Spectrum f represents the

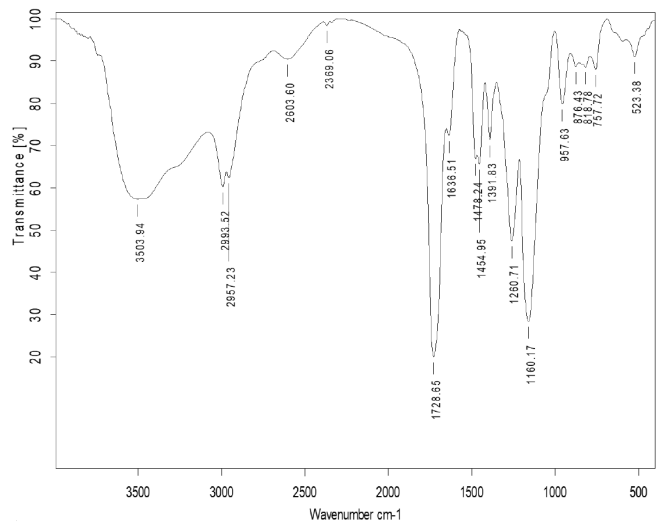

(A)

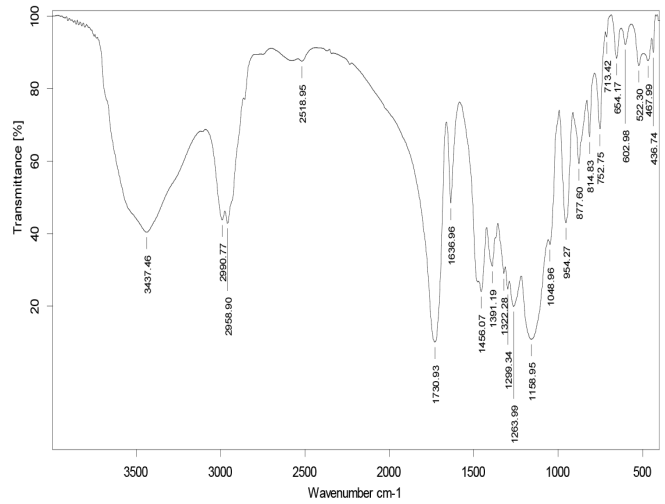

(B)

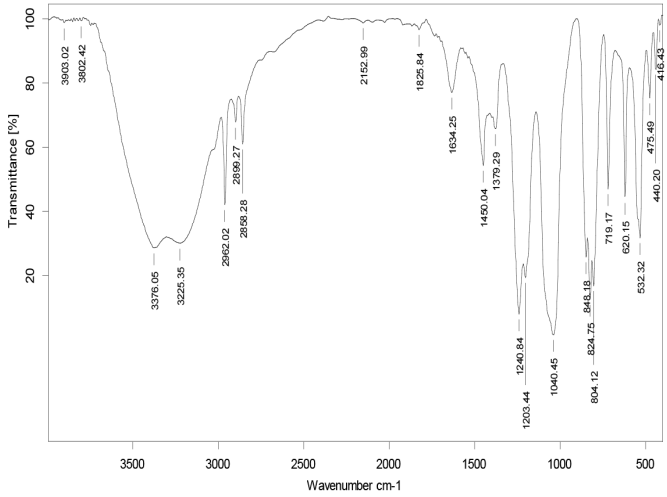

(C)

Fig. 2. Infrared characterization of polymers and pesticides. Infrared characterization of polymers and pesticides. Note: (A) Molecularly imprinted polymer; (B) non-imprinted polymer; (C) trichlorfon.

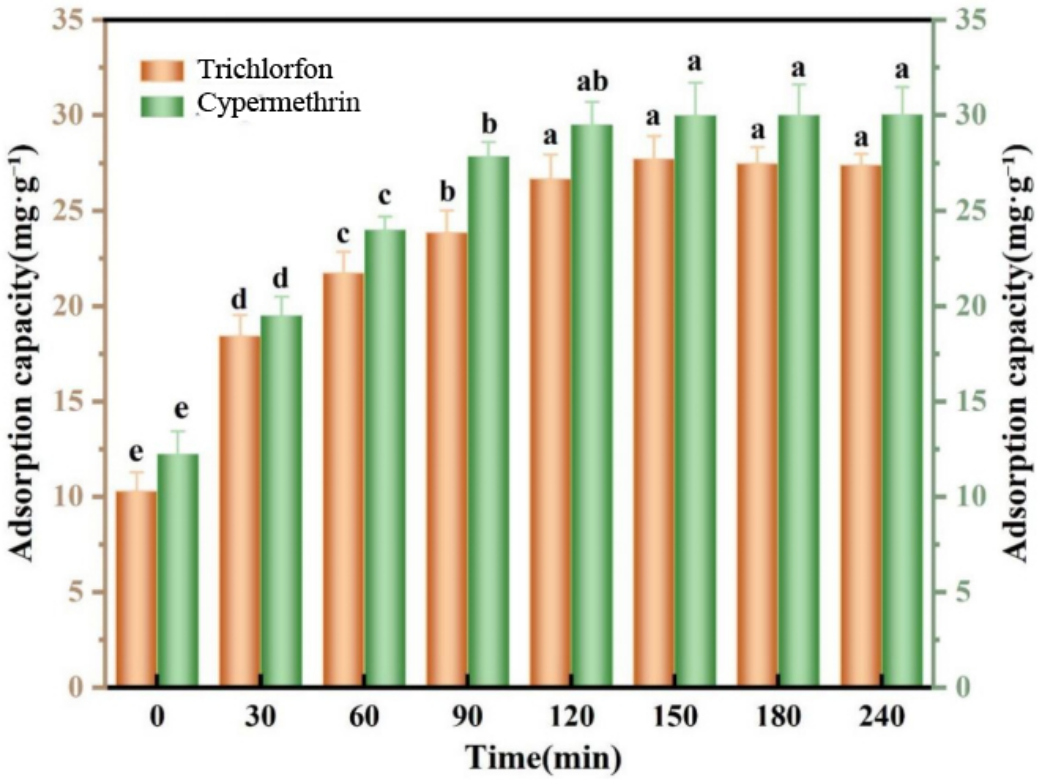

Fig. 3. Kinetic uptake plots of the imprinted polymer towards trichlorfon and cypermethrin at 300 mg/L. Kinetic uptake plots of the imprinted polymer towards trichlorfon and cypermethrin at 300 mg/L. Note: Lowercase letters indicate a 0.05 significance level.

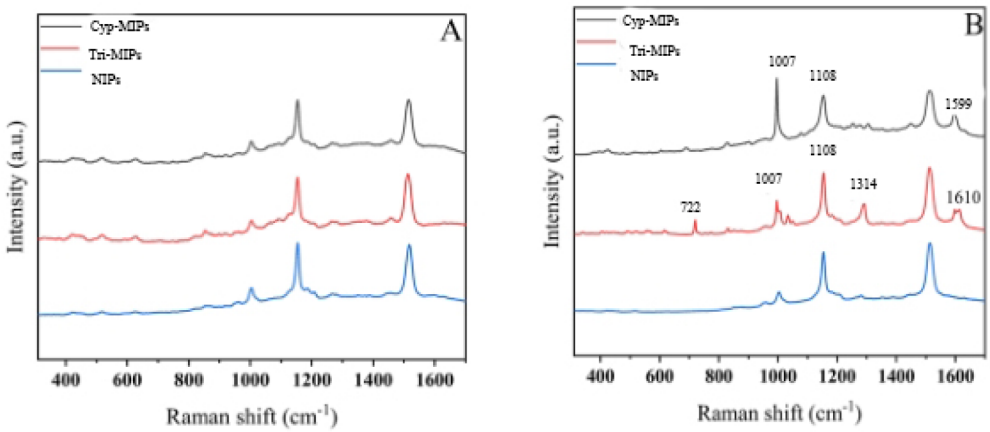

Fig. 4. SEM images of MIP and non-MIP. (A) Raman spectra of Cyp-MIPs adsorb Cypermethrin, Tri-MIPs adsorb Trichlorfon, NIPs adsorb mixed solution. (B) Raman spectra of CIPC-MIPs adsorb CIPC, OPP-MIPs adsorb OPP, NIPs adsorb high concentration mixed solution. MIP, molecularly imprinted polymer; NIP, non-imprinted polymer; CIPC, Chlorpropham; OPP, O-Phenylphenol.

blank control containing only Tri-MIPs and AgNPs. Distinct characteristic peaks of trichlorfon were observed at 712 cm^{-1}, 988 cm^{-1}, 1286 cm^{-1}, and 1598 cm^{-1}. Compared with the standard solution, slight shifts in peak positions and reduced SERS signal intensities were observed. For instance, the characteristic peak at 1286 cm^{-1} shifted by 6 cm^{-1} relative to that of the standard solution, and its intensity was also reduced. These changes primarily arose from non-specific functional groups present in the leeks adsorbing onto the active surface of the AgNPs, thereby interfering with the interaction between the trichlorfon molecules and the AgNPs [35,36]. Nevertheless, the SERS characteristic peaks of trichlorfon in leeks remained clearly distinguishable. In particular, the peak at 1286

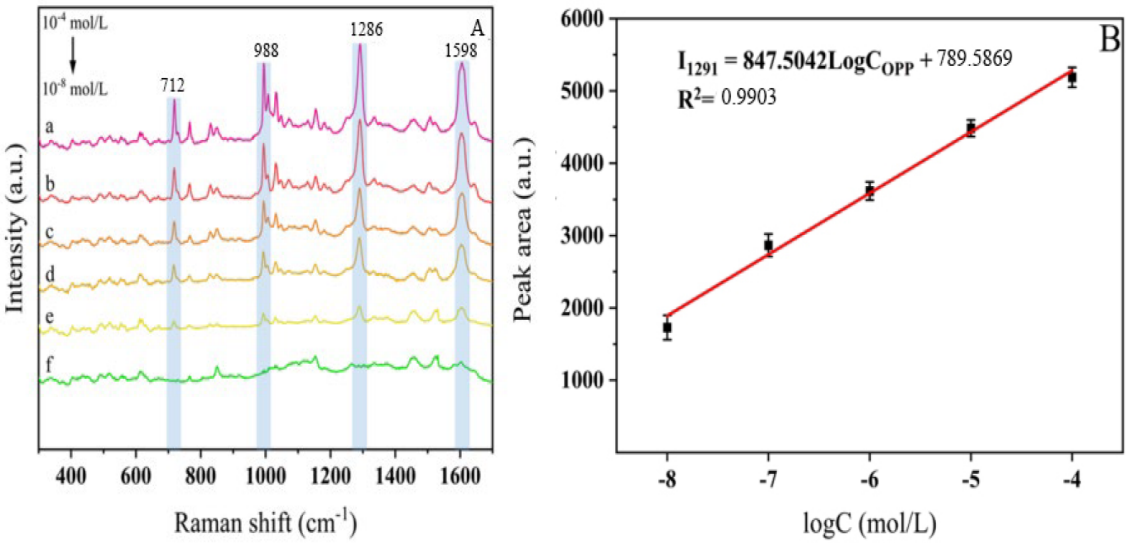

Fig. 5. FTIR spectra of polymers and trichlorfon. (A) SERS spectra of trichlorfon solution with various concentrations on leek. From a to e: 1×10^{-4}, 1×10^{-5}, 1×10^{-6}, 1×10^{-7}, 1×10^{-8} mol/L, f: SERS spectrum of blank control food. (B) The linear correlation diagram between SERS peak intensity at 1286 cm^{-1} of leek and the logarithmic concentration of trichlorfon. SERS, surface-enhanced Raman spectroscopy.

cm^{-1} exhibited distinct characteristics, and its intensity showed a strong linear relationship with concentration. As shown in Fig. 5B, the linear concentration range exhibits good linearity between 1×10^{-8} and 1×10^{-4} mol/L (R^2 = 0.9903). This method is therefore suitable for the quantitative detection of trichlorfon residues in leeks.

As shown in Fig. 6A, spectra a–g represents the SERS spectra of cypermethrin spiked into leeks at concentrations ranging from 1×10^{-3} mol/L to 1×10^{-9} mol/L, while spectrum h is obtained solely from Cyp-MIPs and AgNPs. Distinctive characteristic peaks of cypermethrin were observed at 995 cm^{-1} and 1580 cm^{-1}; these peaks gradually diminished in intensity as the cypermethrin concentration decreased. Overall, the characteristic peaks of cypermethrin remained clearly discernible, with signal intensity decreasing proportionally with concentration. At the same concentration, the SERS signal intensity of cypermethrin was weaker than that observed in the standard solution. This can be attributed to chlorophyll and other components in the leeks competing with cypermethrin molecules for the limited active sites on the AgNP substrate, thereby reducing the overall SERS enhancement effect. Within the concentration range of 1×10^{-9} to 1×10^{-3} mol/L, the intensity of the characteristic Raman peaks exhibited a strong linear relationship with concentration (R^2 = 0.9908), thus providing a reliable basis for the quantitative analysis of cypermethrin residues in leeks (Fig. 6B).

3.4 Calculation of Enhancement Factors

To determine the enhancement effect of AgNPs on the pesticides trichlorfon and cypermethrin, enhancement factors were calculated based on the most prominent characteristic peaks of the two pesticides at 1286 cm^{-1} and 995 cm^{-1}, respectively. Following the procedures described above, optimal enhancement substrates for each pesticide were prepared, and their SERS spectral signals were acquired. For trichlorfon, the surface-enhanced Raman spectroscopy detection limit (CSERS) was 1.1×10^{-5} mol/L, while the conventional Raman detection limit (CNR) was 1 mol/L. Calculations revealed an enhancement factor of 1.62×10^6 for the prepared AgNPs toward trichlorfon, indicating a significant enhancement effect. For the cypermethrin molecule, the surface-enhanced Raman threshold concentration (CRaman) was 1 mol/L, with a threshold ratio (INR) of 270.23 (a.u.). Calculations yielded an enhancement factor of 3.12×10^7 for the prepared AgNPs toward cypermethrin, indicating that the AgNPs substrate exhibits favorable enhancement effects.

3.5 Recovery Rate and Relative Standard Deviation (RSD)

To validate the accuracy and precision of the calibration curves for various practical samples, three different concentrations of trichlorfon and cypermethrin standard solutions (2 µg/L, 5 µg/L, and 10 µg/L) were added to each of the four samples mentioned above. with eight parallel replicates for each concentration. After adsorption onto MIPs, the samples were enhanced using an AgNPs substrate. SERS spectra were collected, and corresponding concentrations were calculated by integrating the characteristic peak intensity into the standard curve. Recovery rates and RSD were calculated for each of the four fruit and vegetable matrices. Results are shown in Table 1. Recovery rates for oranges ranged from 95.2% to 101.4% with RSDs of 3.1% to 7.5%; for mandarins, 97.2% to 101.3%

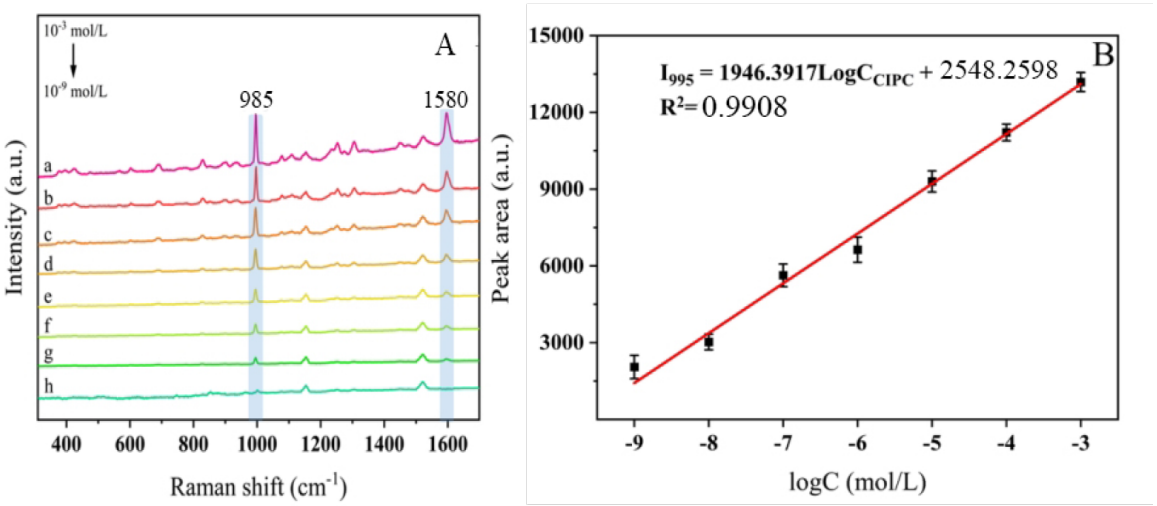

Fig. 6. Kinetic uptake plots of MIP towards pesticides. (A) SERS spectra of cypermethrin solution with various concentrations on Chinese chives. From a to g: 1×10^{-3}, 1×10^{-4}, 1×10^{-5}, 1×10^{-6}, 1×10^{-7}, 1×10^{-8}, 1×10^{-9} mol/L, h: SERS spectrum of blank control food. (B) The linear correlation diagram between SERS peak intensity at 995 cm^{-1} of Chinese chives.

Table 1. Recovery and RSD of Tri and Cyp in four samples (n = 8).

Sample	2 μg/L		5 μg/L		10 μg/L	
	Recovery/%	RSD/%	Recovery/%	RSD/%	Recovery/%	RSD/%
Oranges	95.2%	7.5%	101.4%	3.5%	98.1%	3.1%
Mandarins	97.2%	2.0%	97.5%	1.4%	101.3%	4.3%
Leeks	95.2%	3.1%	98.1%	2.8%	97.6%	2.3%
Spinach	96.1%	5.0%	100.3%	3.9%	98.7%	3.2%

RSD, Relative Standard Deviation.

Table 2. Comparison of methods in this paper with other reported methods.

Pesticide	Method	LOD	LOQ	Reference
Tri	SERS-MIP	1.27 μg/kg	1.67 μg/kg	This work
	LC-MS/MS	0.2 mg/kg	1 mg/kg	Yoshimitsu *et al*., 2020 [37];
	GC-MS/MS	2 μg/kg	10 μg/kg	Liu *et al*., 2021 [38];
Cyp	SERS-MIP	0.13 μg/kg	0.22 μg/kg	This work
	LC-MS/MS	0.14 μg/kg	0.43 μg/kg	Gomes *et al*., 2022 [39];
	GC-MS/MS	2.5 μg/kg	3 μg/kg	Yang *et al*., 2022 [40];

LOD, Limit of Detection; LOQ, Limit of Quantitation; SERS-MIP, molecularly imprinted polymer technology with surface-enhanced Raman spectroscopy; LC-MS/MS, liquid chromatography tandem mass spectrometry; GC-MS/MS, Gas Chromatography-Mass Spectrometry.

with RSDs of 1.4% to 4.3%; leeks showed recovery rates of 95.2%–98.1% with RSDs of 2.3%–3.1%; spinach exhibited recovery rates of 96.1%–100.3% with RSDs ranging from 3.2% to 5.0%. All four samples exhibited satisfactory recovery rates and low RSD values, yielding calibration curves with excellent accuracy. The experimental results comply with the requirements of national standards for physicochemical testing, indicating that the MIPs combined with SERS detection is suitable for the quantitative determination of trichlorfon and cypermethrin in real samples.

3.6 Comparison With Other Detection Methods

The MIP coupled with SERS detection method established in this study was compared with other reported methods for detecting trichlorfon and cypermethrin, with results shown in Table 2 (Ref. [37–40]). It can be seen that the SERS-MIP technology developed in this study exhibits high sensitivity for detecting both pesticides. It requires no cumbersome pretreatment, demonstrates strong specificity and high sensitivity in complex real-world systems, and necessitates only minimal sample quantities—covering the

laser spot suffices for detection. This significantly reduces economic costs. Utilizing a portable Raman spectrometer enables real-time, rapid detection in outdoor settings.

4. Limitation

This study utilized specific surface-enhanced Raman scattering combined with molecularly imprinted polymer (SERS-MIP) technology to detect carbaryl and cypermethrin pesticide residues in four types of fruits and vegetables. Although preliminary success has been achieved, extensive further experimentation is still required. Building on the existing research, the following areas of work can be pursued: (1) In SERS spectral analysis, relying solely on manual interpretation of peak positions and intensities is prone to errors; therefore, it is necessary to develop computational modeling to replace manual analysis and achieve greater precision. (2) This study focused on four common fruits and vegetables; however, given the scope of the pesticide residue issue, testing should be expanded to include a wider range of food products. Additionally, the SERS-MIP technique should be applied to the detection of other types of pesticide residues to establish a comprehensive detection system.

5. Conclusion

Molecularly imprinted polymers (MIPs) were synthesised via precipitation polymerisation using trichlorfon or cypermethrin as the template molecule, methacrylic acid as the functional monomer, acetonitrile and methanol as porogens, azobisisobutyronitrile as the initiator, and divinylbenzene or ethylene glycol dimethacrylate as the crosslinkers. SEM characterisation of the polymers revealed that both Cyp-MIPs and Tri-MIPs exhibited substantially higher specific surface area than the corresponding NIPs. A rapid SERS detection method incorporating pretreatment with Cyp-MIPs and Tri-MIPs was successfully established. Spiked tests were conducted on real samples of oranges, tangerines, leeks, and spinach using the prepared MIPs and AgNPs. Through spiked testing and quantitative analysis of four fruits and vegetables to establish standard curves, the detection results for trichlorfon and cypermethrin pesticides demonstrated good accuracy and reproducibility.

Availability of Data and Materials

All data generated or analyzed during this study are included in this published article.

Author Contributions

ST: Conceptualization. HC: Validation; Data Curation. GHT: Investigation. HRC: Methodology. QAM: Writing – review & editing; Formal Analysis. All authors contributed to editorial changes in the manuscript. All authors read and approved the final manuscript. All authors have participated sufficiently in the work and agreed to be accountable for all aspects of the work.

Ethics Approval and Consent to Participate

Not applicable.

Acknowledgment

Not applicable.

Funding

This study was funded by Hainan Province Natural Science Fund Project (823MS172).

Conflict of Interest

The authors declare no conflict of interest.

References

[1] Gao W, Wan F, Ni W, Wang S, Zhang M, Yu J. Electrochemical Sensor for Detection of Trichlorfon Based on Molecularly Imprinted Sol–Gel Films Modified Glassy Carbon Electrode. Journal of Inorganic and Organometallic Polymers and Materials. 2012; 22: 37–41. https://doi.org/10.1007/s10904-011-9593-4.

[2] Hong X, Qu J, Chen J, Cheng S, Wang Y, Song L, *et al*. Effects of trichlorfon on progesterone production in cultured human granulosa–lutein cells. Toxicology in Vitro. 2007; 21: 912–918. https://doi.org/10.1016/j.tiv.2007.01.016.

[3] Li S, Luo J, Wu Y, Ma X, Pang C, Wang M, *et al*. Determination of trichlorfon using a molecularly imprinted electrochemiluminescence sensor on multi-walled carbon nanotubes decorated with silver nanoparticles. Microchimica Acta. 2022; 189: 347. https://doi.org/10.1007/s00604-022-05452-w.

[4] Ma Y, Li B, Ke Y, Zhang Y. Effects of low doses Trichlorfon exposure on Rana chensinensis tadpoles. Environmental Toxicology. 2019; 34: 30–36. https://doi.org/10.1002/tox.22654.

[5] Hong D, Wang C, Gao L, Nie C. Fundamentals, Synthetic Strategies and Applications of Non-Covalently Imprinted Polymers. Molecules (Basel, Switzerland). 2024; 29: 3555. https://doi.org/10.3390/molecules29153555.

[6] Iacob BC, Bodoki AE, Da Costa Carvalho DF, Serpa Paulino AA, Barbu-Tudoran L, Bodoki E. Unlocking New Avenues: Solid-State Synthesis of Molecularly Imprinted Polymers. International Journal of Molecular Sciences. 2024; 25: 5504. https://doi.org/10.3390/ijms25105504.

[7] Kaspute G, Ramanavicius A, Prentice U. Molecular Imprinting Technology for Advanced Delivery of Essential Oils. Polymers. 2024; 16: 2441. https://doi.org/10.3390/polym16172441.

[8] Li D, Luo K, Zhang L, Gao J, Liang J, Li J, *et al*. Research and Application of Highly Selective Molecular Imprinting Technology in Chiral Separation Analysis. Critical Reviews in Analytical Chemistry. 2023; 53: 1066–1079. https://doi.org/10.1080/10408347.2021.2002680.

[9] Liu Z, Gong A, Qiu L, Liu Y, Zheng S, Qin W, *et al*. Advances in high abundance protein molecular imprinting techniques in human serum. Australian Journal of Chemistry. 2023; 76: 150–168. https://doi.org/10.1071/CH22223.

[10] Lusina A, Cegłowski M. Molecularly Imprinted Polymers as State-of-the-Art Drug Carriers in Hydrogel Transdermal Drug Delivery Applications. Polymers. 2022; 14: 640. https://doi.org/10.3390/polym14030640.

[11] Neng J, Wang J, Wang Y, Zhang Y, Chen P. Trace analysis of food by surface-enhanced Raman spectroscopy combined with molecular imprinting technology: Principle, application, challenges, and prospects. Food Chemistry. 2023; 429: 136883. https://doi.org/10.1016/j.foodchem.2023.136883.

[12] Ratautaite V, Samukaite-Bubniene U, Plausinaitis D, Boguzaite

R, Balciunas D, Ramanaviciene A, *et al*. Molecular Imprinting Technology for Determination of Uric Acid. International Journal of Molecular Sciences. 2021; 22: 5032. https://doi.org/10.3390/ijms22095032.

[13] Sun B, Sun W, Wang Z, Zhao B, Yang S. Highly sensitive electrochemical detection of melatonin based on graphene-assisted molecular imprinting technology. Carbon Letters. 2024; 34: 437–444. https://doi.org/10.1007/s42823-023-00504-4.

[14] Tian R, Li Y, Xu J, Hou C, Luo Q, Liu J. Recent development in the design of artificial enzymes through molecular imprinting technology. Journal of Materials Chemistry. B. 2022; 10: 6590–6606. https://doi.org/10.1039/d2tb00276k.

[15] Xu S, Xu Z, Liu Z. Paper-Based Molecular-Imprinting Technology and Its Application. Biosensors. 2022; 12: 595. https://doi.org/10.3390/bios12080595.

[16] Ye K, Xu S, Zhou Q, Wang S, Xu Z, Liu Z. Advances in Molecular Imprinting Technology for the Extraction and Detection of Quercetin in Plants. Polymers. 2023; 15: 2107. https://doi.org/10.3390/polym15092107.

[17] Yu H, Cai Y, Li Q, Bi S, Huang D. Study on decomposed products of trichlorfon in process of gas chromatographic analysis by mass spectrometry. Chinese Journal of Chromatography. 2006; 24: 23–25. (In Chinese)

[18] European Food Safety Authority (EFSA). Statement on MRLs for alpha-cypermethrin and screening of the existing EU MRLs for cypermethrin. European Food Safety Authority. 2025; 23: e9386. https://doi.org/10.2903/j.efsa.2025.9386.

[19] Li X, Ping X, Xiumei S, Zhenbin W, Liqiang X. Toxicity of cypermethrin on growth, pigments, and superoxide dismutase of Scenedesmus obliquus. Ecotoxicology and Environmental Safety. 2005; 60: 188–192. https://doi.org/10.1016/j.ecoenv.2004.01.012.

[20] Lin HM, Gerrard JA, Shaw IC. Stability of the insecticide cypermethrin during tomato processing and implications for endocrine activity. Food Additives and Contaminants. 2005; 22: 15–22. https://doi.org/10.1080/02652030400027938.

[21] Lin L, Dong T, Nie P, Qu F, He Y, Chu B, *et al*. Rapid determination of thiabendazole pesticides in rape by surface enhanced Raman spectroscopy. Sensors, 2018; 18: 1082. https://https://doi.org/10.3390/s18041082.

[22] Yilmaz EG, Küçük BN, Aslan Y, Erdem Ö, Saylan Y, Inci F, *et al*. Theranostic advances and the role of molecular imprinting in disease management. iScience. 2025; 28: 112186. https://doi.org/10.1016/j.isci.2025.112186.

[23] Yuksel N, Tektas S. Molecularly imprinted polymers: preparation, characterisation, and application in drug delivery systems. Journal of Microencapsulation. 2022; 39: 176–196. https://doi.org/10.1080/02652048.2022.2055185.

[24] Zhang Y, Zhao G, Han K, Sun D, Zhou N, Song Z, *et al*. Applications of Molecular Imprinting Technology in the Study of Traditional Chinese Medicine. Molecules (Basel, Switzerland). 2022; 28: 301. https://doi.org/10.3390/molecules28010301.

[25] Zhao C, Ren Y, Li G. Detection of naringin by fluorescent polarization molecularly imprinted polymer. Polymer Bulletin. 2023; 80: 1411–1424. https://doi.org/10.1007/s00289-022-04115-3.

[26] Zhong L, Zhai J, Ma Y, Huang Y, Peng Y, Wang YE, *et al*. Molecularly Imprinted Polymers with Enzymatic Properties Reduce Cytokine Release Syndrome. ACS Nano. 2022; 16: 3797–3807. https://doi.org/10.1021/acsnano.1c08297.

[27] Zhou Q, Xu Z, Liu Z. Molecularly Imprinting-Aptamer Techniques and Their Applications in Molecular Recognition. Biosensors. 2022; 12: 576. https://doi.org/10.3390/bios12080576.

[28] Akgönüllü S, Denizli A. Molecular imprinting-based sensors: Lab-on-chip integration and biomedical applications. Journal of Pharmaceutical and Biomedical Analysis. 2023; 225: 115213. https://doi.org/10.1016/j.jpba.2022.115213.

[29] Byun HS, Chun D, Shim WG. Separation and recognition characteristics by MIP manufacture using supercritical CO2 technology. Journal of Industrial and Engineering Chemistry. 2021; 97: 356–367. https://doi.org/10.1016/j.jiec.2021.02.021.

[30] Li J, Feng S, Shi T, Wang Y, Liu G. Theoretical study of surface-enhanced Raman spectroscopy of dimethyl methylphosphonate. Spectroscopy Letters. 2025; 58: 161–171. https://doi.org/10.1080/00387010.2024.2422612.

[31] Mueller NS, Pfitzner E, Okamura Y, Gordeev G, Kusch P, Lange H, *et al*. Surface-Enhanced Raman Scattering and Surface-Enhanced Infrared Absorption by Plasmon Polaritons in Three-Dimensional Nanoparticle Supercrystals. ACS Nano. 2021; 15: 5523–5533. https://doi.org/10.1021/acsnano.1c00352.

[32] Tang X, Wu T, Wang C, Zeng W, Ji C, Wei J, *et al*. A three-in-one strategy of molecularly imprinted polymers-based electrochemical SERS for sensitive detection of acetamiprid in vegetables. Food Chemistry. 2025; 476: 143439. https://doi.org/10.1016/j.foodchem.2025.143439.

[33] Xia L, Li G. Recent progress of microfluidics in surface-enhanced Raman spectroscopic analysis. Journal of Separation Science. 2021; 44: 1752–1768. https://doi.org/10.1002/jssc.202001196.

[34] Malakhovsky PO, Ramanenka AA, Artemyev MV. Amplification of the Surface-Enhanced Raman Scattering Signal from a Monolayer of Organic Molecules in Sandwich Structures Containing Plasmonic Silver Nanoplates. Journal of Applied Spectroscopy. 2024; 91: 1010–1016. https://doi.org/10.1007/s10812-024-01814-9.

[35] Usman M, Ishafaq MUU, Muhammad Z, Ali W, Dastgeer G, Zhang X, *et al*. Evaporation-induced self-assembly of gold nanorods on a hydrophobic substrate for surface enhanced Raman spectroscopy applications. Frontiers in Materials. 2023; 9: 1048011. https://doi.org/10.3389/fmats.2022.1048011.

[36] McCabe SM, Gardiner H, Mullen C, Wallace GQ, Shand NC, Mullen AB, *et al*. Live chicken egg embryos as an alternative *in vivo* tumour model for deep surface enhanced Raman spectroscopy. The Analyst. 2024; 149: 3513–3517. https://doi.org/10.1039/d4an00617h.

[37] Yoshimitsu M, Ueno R, Matsui H, Osakada M, Uchida K, Fukui N, *et al*. Development of an LC-MS/MS-Based Rapid and Simple Analytical Method for Six Fungicides. Journal of the Food Hygienic Society of Japan, 2020; 61: 143–147. https://doi.org/10.3358/shokueishi.61.143. (In Japanese)

[38] Liu S, Bai A, Song L, Zou N, Han Y, Zhou L, *et al*. Utilizing a Rapid Multi-Plug Filtration Cleanup Method for 72 Pesticide Residues in Grape Wines Followed by Detection with Gas Chromatography Tandem Mass Spectrometry. Foods. 2021; 10: 2731. https://doi.org/10.3390/foods10112731.

[39] Gomes TM, Perestrelo R, Câmara JS. µQuEChERS Combined with UHPLC-PDA as a State-of-the-Art Analytical Approach for Quantification of Chlorpropham in Potato. Separations, 2022; 9: 77. https://doi.org/10.3390/separations9030077.

[40] Yang L, Huang X, Zeng X, Yi Z. Determination of chlorpropham residues in animal-derived foods by solid phase extraction and ultra-high performance liquid chromatography-tandem mass spectrometry. Chinese Journal of Chromatography, 2022; 40: 41–47. https://doi.org/10.3724/SP.J.1123.2021.02009. (In Chinese)